Supporting Information

Molecular Packing in Two Bicontinuous $Ia\overline{3}d$ Gyroid Phases of Calamitic Cubic Mesogen BABH(n); Roles in Structural Stability and Reentrant Behavior

Yasuhisa Yamamura, Yuri Nakazawa, Shoichi Kutsumizu, and Kazuya Saito

Experimental details

Synthesis of BABH(19)

Materials. *n*-Nonadecan-1-ol (>98.0%) was purchased from Tokyo Chemical Industry Co., Ltd. Carbon tetrabromide (98%, guaranteed reagent), K_2CO_3 (99.5%, guaranteed reagent), NaOH (97%, guaranteed reagent), and $CDCl_3$ (99.8%) were from Nacalai Tesque, Inc., and triphenylphosphine (organics grade), acetone (extra-pure reagent), dichloromethane (guaranteed reagent), *n*-hexane (extra-pure reagent), 2-propanol (extra-pure reagent), tetrahydrofuran (THF, extra-pure reagent), and $CHCl_3$ (extra-pure reagent) were obtained from Kanto Chemical Co., Inc. Thionyl chloride (90%) was purchased from Kishida Chemical Co., Ltd. All starting materials and solvents were used without further purification unless otherwise noted.

Characterization. The purity and characterization of all intermediary compounds and the final compounds were checked by a combination of thin-layer chromatography (TLC: on silica gel coated glass plates (Merck) with fluorescent indicator), NMR spectroscopy, and elemental analysis. ^1H NMR (400 MHz) spectra were recorded on a JEOL FT-NMR spectrometer α-400: $CDCl_3$ was used as solvents and tetramethylsilane (TMS) was used as internal standard ($\delta = 0.00$). Chemical shifts are reported as δ in parts per million downfield from TMS. Elemental analyses were carried out using an elementar micro elemental analyzer UNICUBE at Chemical Analysis Division, Research Facility Center for Science and Technology, University of Tsukuba.

Phase transitions were determined by using a Seiko Denshi DSC-5200. The measurements were performed under a dry N_2 flow of ca. 40 mL min^{-1} and the scanning rate was 5 K min^{-1}. The texture of each mesophase was observed usually under crossed polarizers using a polarizing optical microscope (POM; a Nikon Optiphot-pol XTP-11) equipped with a Mettler FP82 hot stage. The scanning rate was 5 K min^{-1}.

1.1 Preparation of 1-bromo-n-nonadecane[S1]

n-Nonadecan-1-ol (5.00 g, 18 mmol), carbon tetrabromide (6.42 g, 19 mmol), and triphenylphosphine (4.60 g, 18 mmol) were dissolved in anhydrous dichloromethane (70 mL) and stirred at room temperature for 22 h. After the evaporation of the solvent, to the resulting pale yellow liquid was added *n*-hexane (100 mL) and the precipitate was removed by filtration. This procedure was repeated three times and the final filtrate was evaporated to remove the solvent to give a reddish brown solid. The obtained solid was washed with hexane and further purified by column chromatography (eluent: *n*-hexane). From the obtained solution, the solvent was removed by evaporation, dried in vacuum for

3 h, to give a white solid (4.71 g, 14 mmol, 78%). ^{1}H NMR (400 MHz, $\mathrm{CDCl_3}$) δ = 0.88 (t, J = 6.4 Hz, 3H, $\mathrm{CH_3}$), 1.26 (m, 30H, $\mathrm{(CH_2)_{15}}$), 1.42 (quin, J = 6.4 Hz, 2H, $\mathrm{CH_2}\mathit{CH_2CH_2Br}$), 1.85 (quin, J = 7.2 Hz, 2H, $\mathrm{CH_2}\mathit{CH_2Br}$), 3.41 (t, J = 6.8 Hz, 2H, $\mathrm{CH_2Br}$).

1.2 Preparation of 4-(n-nonadecyloxy)benzoic acid

Ethyl 4-hydroxybenzoate (0.71 g, 6 mmol), $\mathrm{K_2CO_3}$ (0.77 g, 5.6 mmol), and 1-bromo-*n*-nonadecane (2.35 g, 30 mmol) were dissolved in acetone (100 mL) and refluxed at 60 °C for 4 h while stirring. Then, $\mathrm{K_2CO_3}$ (0.38 g, 2.7 mmol) was added and further refluxed for 44 h. After cooling to room temperature, the precipitate was removed by filtration, and the solvent was removed by evaporation. The obtained product was dissolved in ethanol (60 mL), to which NaOH (0.30 g, 7.5 mmol) dissolved in water (30 mL) was slowly added and the resulting mixture was refluxed for 2 h. After cooled to room temperature, the precipitate was collected by filtration, which was dissolved in hot acetic acid (200 mL). After cooling to room temperature, the precipitate was collected and recrystallized from acetic acid again and from 2-propanol (200 mL). The final white solid was dried under vacuum for 1 d. Yield 65%.

^{1}H NMR (400 MHz, $\mathrm{CDCl_3}$): δ = 0.88 (t, J = 6.6 Hz, 3H, $\mathrm{CH_3}$), 1.26 (m, 32H, $\mathrm{(CH_2)_{15}}$), 1.46 (quin, J = 7.4 Hz, 2H, $\mathrm{CH_2}\mathit{CH_2CH_2O}$), 1.81 (quin, J = 7.1 Hz, 2H, $\mathrm{CH_2}\mathit{CH_2O}$), 4.02 (t, J = 6.6 Hz, 2H, $\mathrm{CH_2}\mathit{O}$), 6.93 (d, J = 8.8 Hz, 2H, Ar-H), 8.03 (d, J = 8.8 Hz, 2H, Ar-H).

1.3 Preparation of 1,2-bis(4′-(n-nonadecyloxy)benzoyl)hydrazine [BABH(19)][S2]

4-(*n*-nonadecyloxy)benzoic acid (0.95 g, 2.3 mmol) and thionyl chloride (20 mL, 275 mmol) were dissolved in distilled tetrahydrofuran (THF) and the mixture was refluxed for 3 h. After that, the remaining thionyl chloride and the solvent was removed under a reduced pressure to give the acid chloride, to which distilled $\mathrm{CHCl_3}$ (80 mL) was added. To this solution was slowly added dropwise 0.08 mL of hydrazine monohydrate (0.082 g, 1.6 mmol) while stirring at room temperature to give a while precipitate. The solution was further stirred for 15 h, and after that, the precipitate was extracted with $\mathrm{CHCl_3}$ (100 mL) and water (100 mL) three times, dried under vacuum to give a white solid. The crude product was further purified by recrystallization from $\mathrm{CHCl_3}$ three times and finally from 2-propanol-benzene (3:1), dried under vacuum for 2 d to give a final white solid (0.256 g, 4.17 mmol, 28 %). ^{1}H NMR (400 MHz, $\mathrm{CDCl_3}$) δ = 0.88 (t, J = 6.3 Hz, 6H, $\mathrm{CH_3}$), 1.27 (m, 64H, $\mathrm{(CH_2)_{16}}$), 1.80 (m, 4H, $\mathrm{CH_2}\mathit{CH_2O}$), 4.01 (t, J = 6.6 Hz, 4H, $\mathrm{CH_2}\mathit{O}$), 6.95 (d, J = 8.8 Hz, 4H, Ar-H), 7.81 (d, J = 8.8 Hz, 4H, Ar-H), 8.94 (s, 2H, NH). Elemental anal. Calcd for $\mathrm{C_{52}H_{88}N_2O_4}$ (%): C, 77.56; H, 11.02; N, 3.48. Found; C, 77.39; H, 10.81; N, 3.55.

Characterization of phase transition behavior of BABH(19)

To characterize the phase behavior of BABH(19), DSC measurement and polarizing microscopic observation (POM) were carried out. The DSC thermogram and microphotographs are shown in Figures S1 and S2, respectively.

The as-grown sample was heated up to ca. 450 K on 1st heating (1H in Figure S1). The cooling DSC thermograms indicated as 1C (1st cooling) and 2C (2nd cooling) in the figure show clear heat anomalies due to two phase transitions: isotropic liquid (Iso) to $Ia\bar{3}d$ cubic ($Ia\bar{3}d$) phases and $Ia\bar{3}d$ to crystalline solid (Cr) phases. Each phase was identified by microscopic observations shown in Figure S2. The phase transition temperatures and enthalpies determined from the DSC thermogram are listed in Table S1.

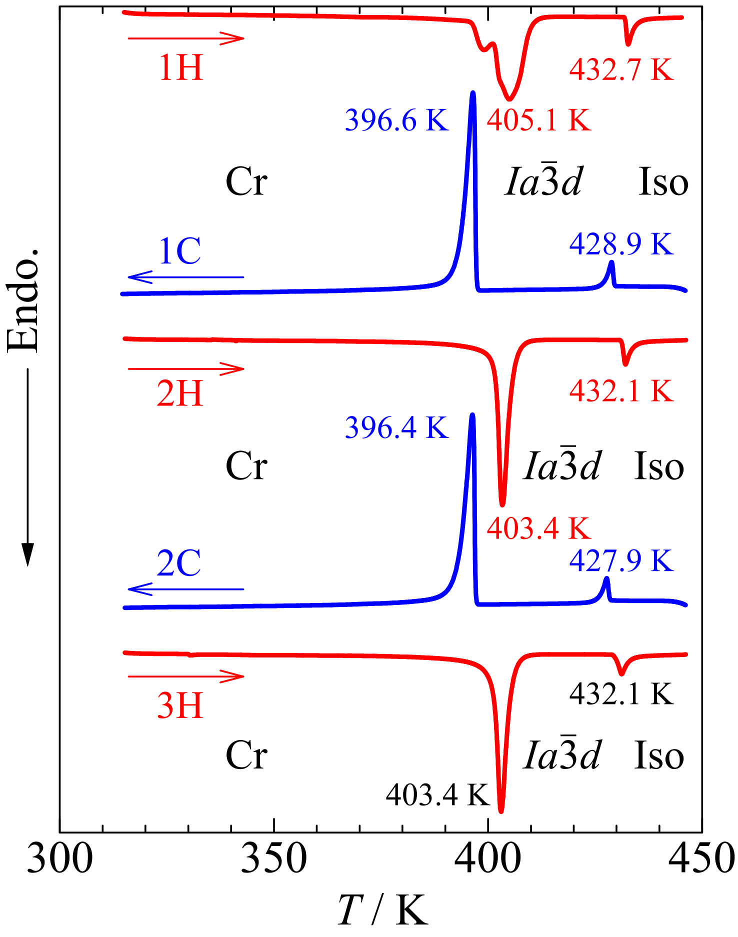

Figure S1. DSC thermogram of BABH(19).

Table S1. Phase transition temperatures (in K) and enthalpies (in kJ mol^{-1} in parentheses) for BABH(19).

run	Cr		$Ia\bar{3}d$		Iso
1H	•	405.1 (125.6)	•	432.7 (10.8)	•
1C	•	396.6 (-110.3)	•	428.9 (-7.2)	•
2H	•	403.4 (107.1)	•	432.1 (9.9)	•
2C	•	396.4 (-107.1)	•	427.9 (-7.1)	•
3H	•	403.4 (107.1)	•	432.1 (9.9)	•

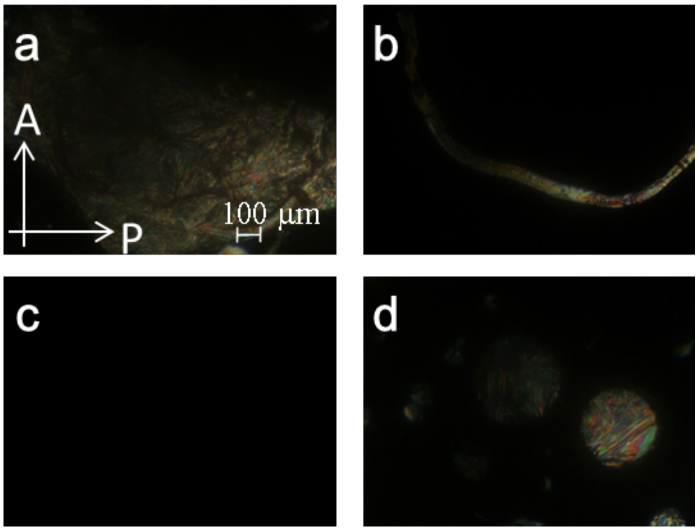

Figure S2. Microphotographs for BABH(19) (a) at 359 K (Cr) and (b) at 405 K (Cr → Cub/$Ia\bar{3}d$) on heating, and (c) at 426 K (Cub/$Ia\bar{3}d$) and (d) at 391 K (Cub/$Ia\bar{3}d$ → Cr) on cooling, as observed under crossed polarizers (P, polarizer; A, analyzer).

X-ray experiments on BABH(17) and BABH(19) and MEM analyses

The small-angle X-ray diffraction (SAXD) experiments were performed for the $Ia\bar{3}d$ phase of BABH(17) and BABH(19) using a Rigaku NANO-Viewer IP system. The Cu Kα radiation (λ = 0.154 nm) was focused with a Confocal Max-Flux mirror and collimated into a sample capillary placed in a heated cell using a three-slit system. The scattered X-rays were recorded on an imaging plate (IP) camera with an effective area of 11.5×11.5 cm^2. The distances between the sample and the IP were 45 cm for all the samples. After the absence of the preferred orientation was ascertained, the intensities were circularly integrated and averaged to yield an intensity versus scattering angle profile using a homemade program. Figure S3 shows the x-ray diffraction patterns of BABH(17) and BABH(19). All the detected peaks were reasonably approximated to a Gaussian line shape and so the peak area and its error were estimated through curve fitting. The Lorentz correction on them yielded the final intensities. The experimental magnitude of the structure factors ($|F(\boldsymbol{q})|$) and errors ($\sigma(F)$) thus estimated are given in Tables S2. Our previous procedure of the MEM analyses was applied to the present cases.[S3] The unit cell was divided into 128 × 128 × 128 pixels. Figure S4 shows the electron density of BABH(19) reconstructed by MEM analysis.

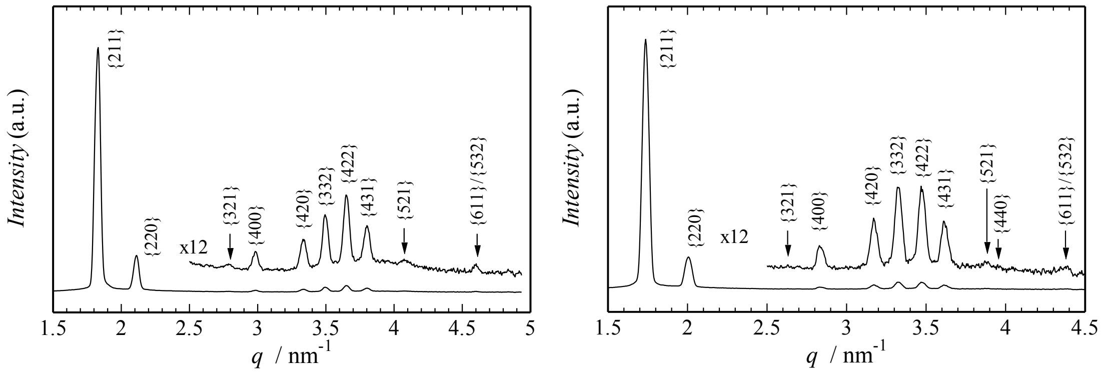

Figure S3. X-ray diffraction patterns of BABH(17) (left) and BABH(19) (right).

Table S2. Experimental and calculated F and $\sigma(F)$ values for BABH(17) and BABH(19). "-" indicates nonobserved reflections within the experimental $|\boldsymbol{q}|$ range.

index	BABH(17)			BABH(19)		
(hkl)	$\lvert F_{obs} \rvert$	F_{cal}	$\sigma(F_{obs})$	$\lvert F_{obs} \rvert$	F_{cal}	$\sigma(F_{obs})$
(211)	1.000	-1.000	0.013	1.000	-1.000	0.006
(220)	0.514	-0.522	0.005	0.507	-0.507	0.005
(321)	0.027	-0.028	0.002	0.012	-0.012	0.001
(400)	0.150	-0.156	0.003	0.171	-0.135	0.006
(420)	0.099	0.101	0.001	0.131	0.130	0.002
(332)	0.132	-0.134	0.002	0.175	-0.175	0.002
(422)	0.157	-0.160	0.001	0.174	-0.172	0.002
(431)	0.082	-0.083	0.001	0.093	-0.093	0.002
(521)	0.039	0.039	0.003	0.032	0.032	0.004
(440)	-	-	-	0.017	0.014	0.010

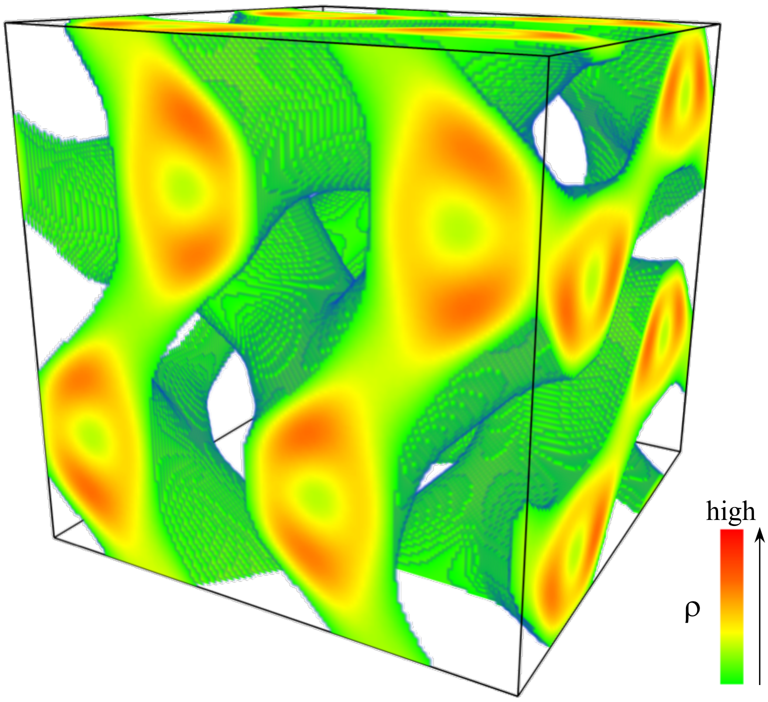

Figure S4. Electron density of BABH(19) reconstructed by MEM analysis [green (medium) to red (high)]. The region with a lower density than the average is shown transparently.

References

[S1] R. Appel, *Angew. Chem. Int. Ed.*, **14**, 801–811 (1975).

[S2] S. Kutsumizu, H. Mori, M. Fukatami, S. Naito, K. Sakajiri, and K. Saito, *Chem. Mater.*, **20**, 3675–3687 (2008).

[S3] Y. Nakazawa, Y. Yamamura, S. Kutsumizu, and K. Saito, *J. Phys. Soc. Jpn.*, **81**, 094601 (2012).